Kank attenuates actin remodeling by preventing interaction between IRSp53 and Rac1

Badal Chandra Roy, Naoto Kakinuma, and Ryoiti Kiyama

Neuroscience Research Institute, National Institute of Advanced Industrial Science and Technology, Tsukuba, Ibaraki 305-8566, Japan

In this study, insulin receptor substrate (IRS) p53 is identified as a binding partner for Kank, a kidney ankyrin repeat–containing protein that functions to suppress cell proliferation and regulate the actin cytoskeleton. Kank specifically inhibits the binding of IRSp53 with active Rac1 ($Rac1^{G12V}$) but not Cdc42 ($cdc42^{G12V}$) and thus inhibits the IRSp53-dependent development of lamellipodia without affecting the formation of filopodia. Knockdown (KD) of Kank by RNA interference results in increased lamellipodial development, whereas KD of both Kank and IRSp53 has little effect. Moreover, insulin-induced membrane ruffling is inhibited by overexpression of Kank. Kank also suppresses integrin-dependent cell spreading and IRSp53-induced neurite outgrowth. Our results demonstrate that Kank negatively regulates the formation of lamellipodia by inhibiting the interaction between Rac1 and IRSp53.

Introduction

The Rho family of small GTPases acts as molecular switches for a variety of extracellular signals (Hall, 1998). These signals are transduced through a rapid reorganization of the actin cytoskeleton that changes the cell shape, leading to cell adhesion and locomotion (Ridley et al., 1992). Rho GTPases are also implicated in many other cellular events and functions such as cell polarity, gene transcription, cell cycle progression in the G1 phase, microtubule dynamics, vesicular transport, and enzymatic processes (Kozma et al., 1996; Van Aelst and D'Souza-Schorey, 1997; Aspenström, 1999; Etienne-Manneville and Hall, 2002). The Rho family proteins such as Rac1 and cdc42 along with proteins like Wiskott-Aldrich syndrome protein (WASP), neural WASP, and Scar/WAVE participate in cell migration, neurite extension, and budding in yeast (Innocenti et al., 2004). These proteins can bind to the globular actin and Arp2/3 complex through their catalytic domain, which results in filament branching at the membrane (Takenawa and Miki, 2001). The regulatory actions of WASP and neural WASP proteins involve their binding to active cdc42 at their GTPase-binding domain (Higgs and Pollard, 2000; Takenawa and Miki, 2001). WAVE1 was found to be inactive in a complex with Nap1, Abi2, PIR121, and HSP300, and a GTP-loaded active Rac1 dissociated from this complex, relieving active WAVE1-HSP300 (Eden et al., 2002). In contrast, WAVE2 was found to bind to active Rac1 indirectly through insulin receptor substrate (IRS) p53 (Miki et al., 2000; Miki and Takenawa, 2002), a well-characterized adapter protein that connects actin remodeling proteins with the Rho family of small GTPases (Funato et al., 2004). IRSp53 contains several domains: a Rac1-binding domain in the N terminus, a half cdc42/Rac1 interactive binding (CRIB) motif, a proline-rich domain, and an Src homology 3 (SH3) domain. It also binds to cdc42 via the CRIB motif and stimulates the formation of filopodia through Mena (Govind et al., 2001; Krugmann et al., 2001). IRSp53 is involved in neuronal morphogenesis through a variety of proteins (Soltau et al., 2002, 2004; Choi et al., 2005; Hori et al., 2005).

During a comprehensive analysis of loss of heterozygosity in renal cell carcinoma patients, Kank, a kidney ankyrin repeat–containing protein, was identified as a growth suppressor in HEK293 cells and a disruptor of β-actin distribution in G-402 cells (Sarkar et al., 2002; Rodley et al., 2003). The protein contains a coiled-coil domain in the N-terminal region and an ankyrin repeat domain in the C-terminal region, both of which are likely to be involved in protein–protein interactions and thus may play a major role in cellular events. Interestingly, an orthologue of Kank in *Caenorhabditis elegans*, VAB-19, was reported to act in epidermal morphogenesis and to play a

B.C. Roy and N. Kakinuma contributed equally to this paper.

Correspondence to Ryoiti Kiyama: kiyama.r@aist.go.jp

Abbreviations used in this paper: CRIB, cdc42/Rac1 interactive binding; esiRNA, endoribonuclease-prepared siRNA; F-actin, filamentous actin; IRS, insulin receptor substrate; KD, knockdown; MBP, maltose-binding protein; mIRS, mouse IRSp53; WASP, Wiskott-Aldrich syndrome protein.

The Rockefeller University Press $30.00
J. Cell Biol. Vol. 184 No. 2 253–267
www.jcb.org/cgi/doi/10.1083/jcb.200805147

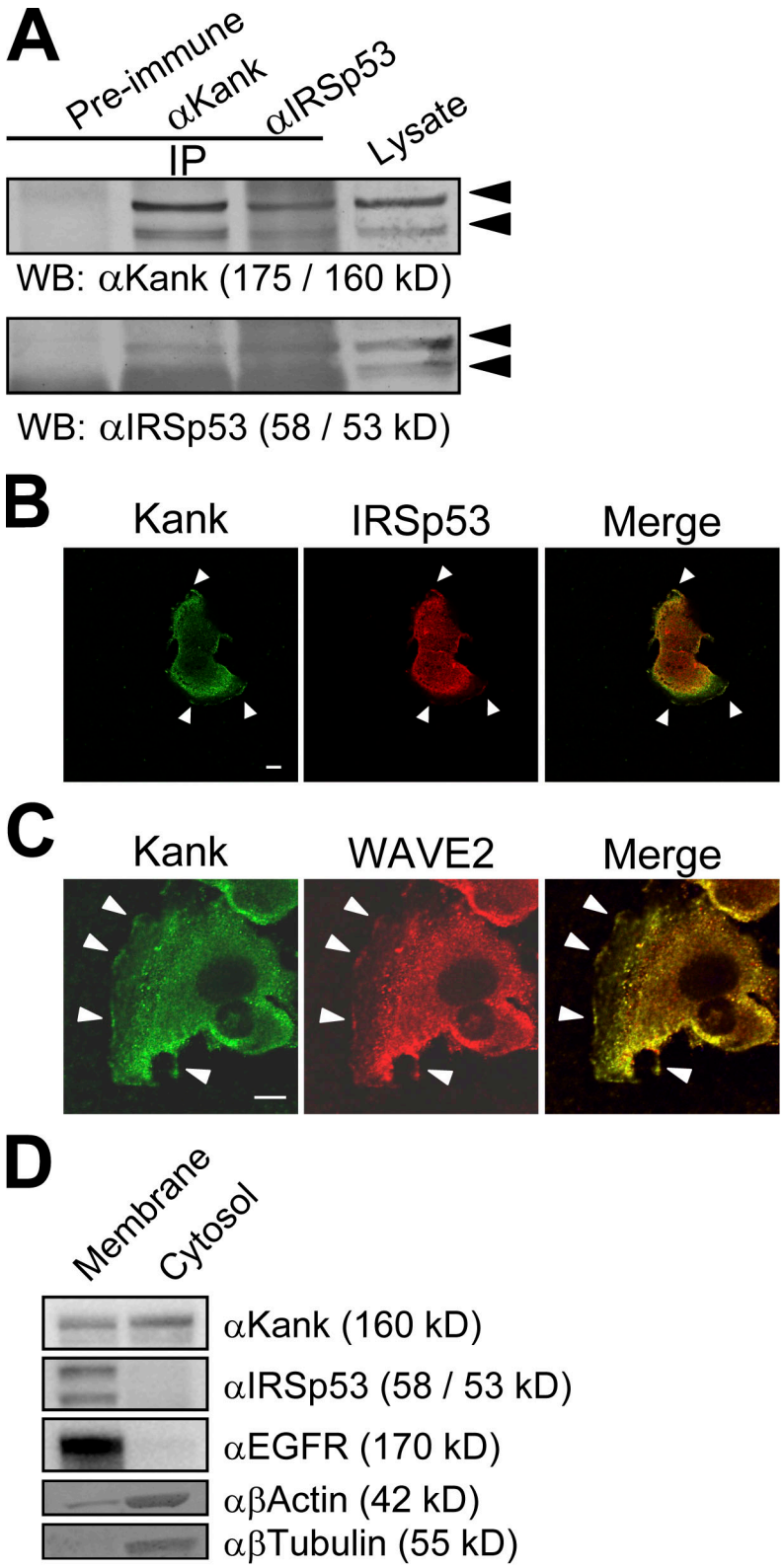

Figure 1. **Kank interacts and is partially colocalized with IRSp53 in vivo.** (A) Coimmunoprecipitation of Kank and IRSp53 in VMRC-RCW cells. Approximately 600 µg of total protein lysate (shown on the right) was used for immunoprecipitation (IP) with a preimmune serum or with a polyclonal antibody against Kank or IRSp53. The proteins in the immunoprecipitates were detected by Western blotting (WB; arrowheads). (B) Immunostaining of Kank and IRSp53 in VMRC-RCW cells. Confocal laser microscopic images were obtained for Kank (green) and IRSp53 (red) using anti-Kank (monoclonal) and anti-IRSp53 (polyclonal) antibodies, respectively, and their colocalization at the cell periphery (arrowheads) is shown in yellow. (C) Immunostaining of Kank and WAVE2 in VMRC-RCW cells. Confocal laser microscopic images were obtained for Kank (green) and WAVE2 (red) using anti-Kank (polyclonal) or anti-WAVE2 (goat polyclonal) antibodies, respectively, and their colocalization at the cell periphery (arrowheads) is shown in a merged image (yellow). (D) Fractionation of HeLa cells. The proteins in the membrane and cytosolic fractions were separated, and those indicated were detected by Western blotting. EGF receptor is a marker for the membrane, and β-actin and β-tubulin are markers for the cytosol. Bars, 10 µm.

significant role in the regulation of the actin cytoskeleton (Ding et al., 2003).

In this study, we report that Kank disrupts the function of active Rac1 through IRSp53. The binding between IRSp53 and Kank inhibits the association of active Rac1 with IRSp53 rather than the association of active cdc42 with IRSp53. Kank inhibits the formation of lamellipodia and membrane ruffles induced by active Rac1 in NIH3T3 cells. In addition, the depletion of Kank induced lamellipodial membrane protrusions in NIH3T3 cells. Furthermore, Kank inhibits IRSp53-induced cell spreading and neurite outgrowth in N1E115 cells.

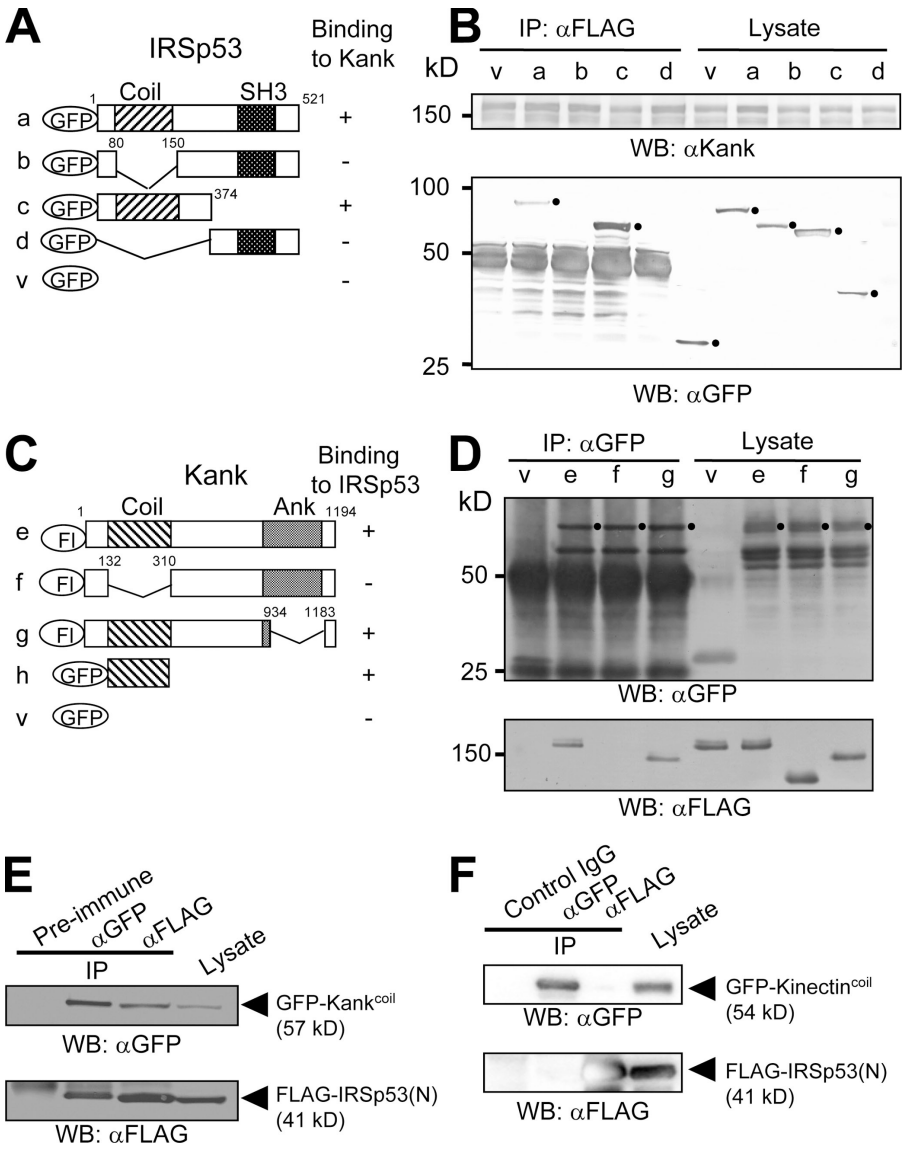

Figure 2. **Kank interacts with IRSp53 through their coiled-coil domains.** (A) GFP-tagged constructs of IRSp53 used in this study and the results of binding to Kank. (B) Interaction of IRSp53 with Kank through its coiled-coil domain. The vectors expressing Flag-Kank and GFP-tagged constructs (constructs a–d in A) of IRSp53 were transfected in HEK293T cells, and the complex containing Kank was immunoprecipitated with an anti-Flag antibody and analyzed by Western blotting using an anti-Kank antibody (top) or an anti-GFP antibody (indicated by dots; bottom). The GFP expression vector was used as a control (v), and the lysate lanes show the expression of each plasmid construct (bottom). (C) Flag-tagged and GFP-tagged Kank constructs used in this study and the results of binding to IRSp53. (D) Interaction of Kank with IRSp53 through its coiled-coil domain. The vectors expressing GFP-IRSp53(N) and Flag-tagged constructs (constructs e–g in C) of Kank were transfected in HEK293T cells, and the complex containing IRSp53(N) was immunoprecipitated with an anti-GFP antibody and analyzed by Western blotting using an anti-GFP antibody (the positions of GFP-IRSp53(N) are indicated by dots; top) or an anti-Flag antibody (bottom). The GFP expression vector was used as a control (v), and the lysate lanes show the expression of each plasmid construct (bottom). (E) Interaction of the coiled-coil domain of Kank with IRSp53. The lysates from the cells expressing the GFP-tagged coiled-coil domain of Kank (Kank^{coil}; construct h in C) and Flag-IRSp53(N) (construct c in A) were immunoprecipitated with preimmune serum or with an antibody against GFP or Flag. The complex was then analyzed by Western blotting. (F) The coiled-coil domain of IRSp53 does not interact with the coiled-coil domain of kinectin. The lysates of the cells expressing the GFP-tagged coiled-coil domain of kinectin (amino acids 1,116–1,356; GFP-kinectin^{coil}) and Flag-IRSp53(N) (construct c in A) were immunoprecipitated with control IgG or antibodies against GFP (α-GFP) or Flag (α-Flag). The complex was then analyzed by Western blotting as indicated. IP, immunoprecipitation; WB, Western blot.

Results

Kank interacts with IRSp53 in vivo

To identify proteins binding to Kank, we screened a human placental cDNA library using Kank (amino acids 77–977) as bait with the yeast two-hybrid system. Among >200 clones isolated, two encoded IRSp53, both lacking 49 amino acids from the N terminus. The specificity of interaction was confirmed by the growth of the yeast clones on plates lacking Leu/Trp/His and by β-galactosidase activity in the X-gal filter assay (unpublished data). To verify the result of the screening, reciprocal coimmunoprecipitation experiments were performed using antibodies against Kank and IRSp53 with mammalian cell lysates (Fig. 1 A). Immunoprecipitation of Kank resulted in the coprecipitation of IRSp53 as detected by Western blotting using the anti-IRSp53 antibody, whereas the result of the control experiment using a preimmune serum was negative. However, immunoprecipitation of IRSp53 resulted in coprecipitation of Kank as detected with the anti-Kank antibody, confirming binding in vivo between Kank and IRSp53. Immunocytochemical characterization of Kank in VMRC-RCW cells, a renal cell carcinoma cell line, also showed the colocalization of endogenous Kank and IRSp53 at the cell periphery (Fig. 1 B, arrowheads). To further authenticate our finding, we coimmunostained Kank with WAVE2, which is known to be localized to areas of ruffling, in VMRC-RCW cells. Kank and WAVE2 were colocalized at the cell periphery (Fig. 1 C, arrowheads). Furthermore, Kank and IRSp53 were both present in the membrane fraction (Fig. 1 D). In the spreading cells, IRSp53 was detected at the tips of both the lamellipodium and the filopodium (Nakagawa et al., 2003) where WAVE2 is also localized (Miki et al., 2000). Thus, we concluded that Kank is localized at the leading edge in the VMRC-RCW cells.

To determine the binding domains of Kank and IRSp53, various mutants were constructed for IRSp53 (in GFP-tagged forms; Fig. 2 A) and Kank (in Flag-tagged forms; Fig. 2 C). HEK293T cells were transfected with the indicated constructs along with the wild-type Flag-Kank, and immunoprecipitation

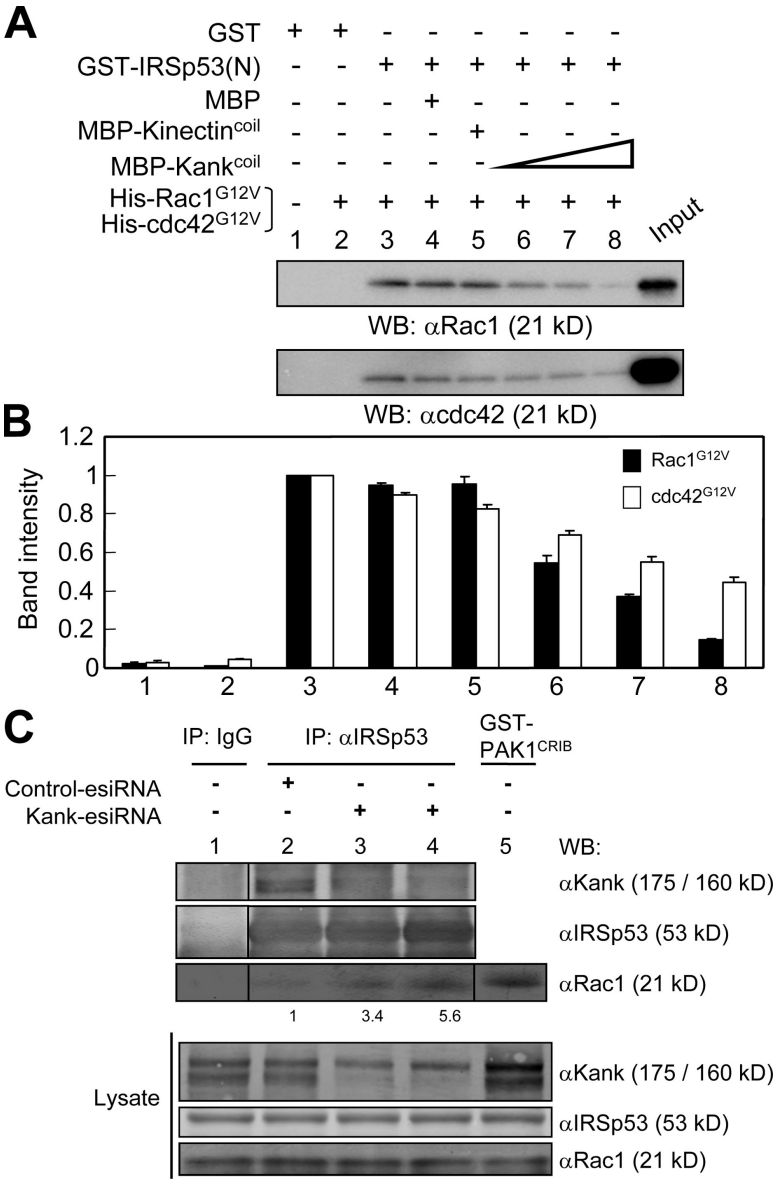

Figure 3. **Kank regulates the binding between IRSp53 and active Rac1.** (A) Inhibition of binding in vitro of Rac1 (for the top Western blots) or cdc42 (for the bottom Western blots) with IRSp53 by Kank. Binding between GST-IRSp53(N) (lanes 3–8) or control GST (lane 1) and His-Rac1^{G12V} or His-cdc42^{G12V} (lanes 2–8) was examined in the presence of MBP-Kank^{coil} (increasing concentrations; lanes 6–8). His-Rac1^{G12V} (top) and His-cdc42^{G12V} (bottom) used for the experiments in lanes 2–8 are shown in the last lane (shown as Input). (B) Quantified data of Rac1 and cdc42 bands. The intensity of the bands of Rac1 and cdc42 in A was quantified, and the mean ± SD of three Western blots for each band is shown. Band intensities are measured in arbitrary units. (C) Increased binding between IRSp53 and active Rac1 in vivo on KD of Kank. Lysates from HEK293 cells stably expressing Rac1^{G12V} were used for immunoprecipitation (IP) with normal IgG as a negative control (lane 1) or with α-IRSp53 (against the C terminus) after transfection with control esiRNA (lane 2) or with Kank esiRNA (lanes 3 and 4, duplicated). Pull down with GST-PAK1^{CRIB}, a cdc42/Rac1-binding domain of PAK1 fused to GST, was used for detecting active Rac1 (lane 5). Western blots of individual proteins are shown. Immunoprecipitated Rac1 and IRSp53 were quantified, and the relative amount of coimmunoprecipitated Rac1 was calculated as the ratio of the intensity of Rac1 to that of corresponding immunoprecipitated IRSp53 and is shown under the image of anti-Rac1 antibody. Black lines indicate that intervening lanes have been spliced out. WB, Western blot.

was performed using an anti-Flag antibody (Fig. 2 B). Positive GFP signals were observed for the wild-type GFP-IRSp53 (Fig. 2 A, construct a) and GFP-IRSp53(N) (N-terminal part containing the IMD/RCB domain and half CRIB domain; Fig. 2 A, construct c). In contrast, a mutant of IRSp53 having a deletion at the coiled-coil domain (amino acids 75–153; GFP-IRSp53$^{\Delta coil}$; Fig. 2 A, construct b), a mutant containing the C-terminal part, including the SH3 domain (amino acids 362–521; construct d), and the GFP-vector (control; Fig. 2 A, construct v) did not show any signal for GFP in the immunoprecipitates, indicating that Kank binds to IRSp53 at its coiled-coil domain. The lanes for lysates showed the expression of the individual constructs. Similarly, Flag-tagged Kank and its mutants were expressed in HEK293T cells along with GFP-IRSp53(N) (Fig. 2 A, construct c) and were immunoprecipitated with polyclonal anti-GFP antibody (Fig. 2 D). Western blotting using an anti-Flag antibody showed strong signals for Flag-Kank (Fig. 2 C, construct e) and Flag-Kank$^{\Delta Ank}$ (Fig. 2 C, construct g) but no signal for Flag-Kank$^{\Delta coil}$ (Fig. 2 C, construct f). The result also indicates that Kank binds to IRSp53 at the coiled-coil domain. This result was further verified by coexpressing Flag-IRSp53(N) (Fig. 2 A, construct c) and a GFP-tagged coiled-coil region of Kank (Fig. 2 C, construct h) in HEK293T cells and by examining reciprocal immunoprecipitation followed by Western blotting (Fig. 2 E). The specificity of the binding was further examined by using a coiled-coil domain of kinectin (amino acids 1,116–1,356; GFP-kinectin^{coil}; Fig. 2 F). In this study, GFP-kinectin^{coil} did not bind to Flag-IRSp53(N). Thus, the results indicate that IRSp53 binds specifically to Kank through its coiled-coil domain.

Kank regulates the binding between active Rac1 and IRSp53

As reported, active Rac1 binds to IRSp53 through its N-terminal 229 amino acid residues (Miki et al., 2000; Miki and Takenawa, 2002), which contain the Kank binding domain, so we tested whether Kank can compete against Rac1 in vitro (Fig. 3, A and B). Both His-Rac1^{G12V} and His-cdc42^{G12V} bound to GST-IRSp53(N), whereas GST alone did not, indicating that IRSp53 binds

to Rac1 or cdc42 (Fig. 3, A and B, lanes 2 and 3). When this binding was challenged by maltose-binding protein (MBP; a control) or MBP-Kank^{coil}, MBP-Kank^{coil} inhibited the binding of GST-IRSp53(N) to His-Rac1^{G12V} in a dose-dependent manner more efficiently than the binding of GST-IRSp53(N) to His-cdc42^{G12V} (Fig. 3, A and B, lanes 6–8). MBP alone or MBP-kinectin^{coil} (containing a control coiled-coil domain) did not affect the binding (Fig. 3, A and B, lanes 4 and 5). In Fig. 2 B, we determined the binding domain of Kank in IRSp53 (amino acids 80–150), which also overlapped with the coiled-coil domain and was located within the RCB. Yamagishi et al. (2004) reported that the N-terminal half of IRSp53 contains a filopodium-inducing domain regulated by Rac1 and cdc42. IRSp53 contains a partial CRIB motif (Burbelo et al., 1995; Govind et al., 2001; Krugmann et al., 2001), a sequence of 16 amino acid residues (amino acids 267–283), which is located far from the Kank binding domain (amino acids 80–150). Our result showed that the binding of Kank to IRSp53 partially affected the binding between cdc42 and IRSp53 (Fig. 3, A and B). We then examined the effect of knockdown (KD) of Kank using endoribonuclease-prepared siRNA (esiRNA) on the binding between active Rac1 and IRSp53 in vivo (Fig. 3 C). For this, we established HEK293 cells stably expressing active Rac1 (Rac1^{G12V}). These cells were transfected with Kank esiRNA along with control esiRNA. After treatment with esiRNA for 30 h, the cells were subjected to immunoprecipitation using an anti-IRSp53 antibody that was raised against the C-terminal portion of IRSp53. The results of Western blot analysis revealed that Kank esiRNA efficiently decreased the level of Kank protein in the lysates but did not change the level of IRSp53 or Rac1 protein (Fig. 3 C, compare lanes 3 and 4 with lanes 1 or 2 in the lysate panel). The results of immunoprecipitation showed that depletion of Kank with Kank esiRNA resulted in less Kank (Fig. 3 C, compare lanes 3 and 4 with lane 2 in the top row) and, at the same time, increased the amount of active Rac1 (Rac1^{G12V}; Fig. 3 C, lanes 2–4 in the third row), both of which were immunoprecipitated with IRSp53. In other words, KD of Kank resulted in increased binding between IRSp53 and active Rac1. Normal IgG was used as a negative control, and GST-PAK1^{CRIB} was used for the pull down of active Rac1 (Fig. 3 C, lanes 1 and 5, respectively). From these results, Kank specifically inhibits the binding of Rac1 to IRSp53.

Kank inhibits Rac1-induced formation of lamellipodia through IRSp53

Kank affected the interaction between IRSp53 and Rac1 and partially affected that between IRSp53 and cdc42 (Fig. 3). This led us to investigate the effect of Kank expression on the formation of lamellipodia or filopodia mediated by Rac1 or cdc42 (Figs. 4 and 5). Initially, IRSp53 was reported to be a downstream target of Rac1 that links Rac1 activity to WAVE/Scar and the Arp2/3 complex (Miki et al., 2000; Etienne-Manneville and Hall, 2002). However, others reported that IRSp53 preferentially binds to active cdc42 (Govind et al., 2001; Krugmann et al., 2001). Overexpression of Kank severely impaired the development of lamellipodia and cell spreading induced by a constitutively active form of Rac1, Rac1^{G12V} (Fig. 4 A, lane 4). Overexpression of Kank^{S167A}, which lacks the ability to bind to 14-3-3 and has inhibitory effects on active RhoA and cell migration (Kakinuma et al., 2008), also impaired the formation of lamellipodia induced by Rac1^{G12V} (Fig. 4 A, lane 5). However, Kank$^{\Delta coil}$, which cannot interact with IRSp53, had no effect on the Rac1^{G12V}-induced development of lamellipodia (Fig. 4 A, lane 6). To confirm that this effect of Kank depends on the interaction with IRSp53, we performed coexpression of Kank with IRSp53 (Fig. 4 B). Coexpression of GFP-Rac1^{G12V} and Kank with IRSp53 resulted in the disappearance of Kank's inhibitory effect on the Rac1^{G12V}-dependent formation of lamellipodia (Fig. 4 B, lane 4). However, coexpression of GFP-Rac1^{G12V} and Kank with IRSp53$^{R11E/Q23E}$ or IRSp53^{K143E}, which could not bind to Rac1 and could bind to Kank (Fig. S1, available at http://www.jcb.org/cgi/content/full/jcb.200805147/DC1; Suetsugu et al., 2006b), resulted in the retention of the inhibitory effect on the Rac1^{G12V}-dependent development of lamellipodia (Fig. 4 B, lanes 5 and 6). This result implies that Kank inhibits Rac1–IRSp53 signals for the formation of lamellipodia. Moreover, to confirm that this Rac1^{G12V}-dependent formation depends on IRSp53, we performed KD of IRSp53 along with GFP-Rac1^{G12V} expression (Fig. 4 C). We first examined the KD of mouse IRSp53 (mIRS) in NIH3T3 cells using various candidate plasmids (Fig. S2). These plasmids contained an H1 promoter–based expression system for siRNAs in mammalian cells (Steffen et al., 2004). Based on the results, we used #513 siRNA for the KD of mIRS. Coexpression of GFP-Rac1^{G12V} and mIRS-KD reduced the Rac1^{G12V}-dependent formation of lamellipodia (Fig. 4 C, lane 3), whereas on the coexpression of human IRSp53 with GFP-Rac1^{G12V} and mIRS-KD, GFP-Rac1^{G12V} retained its function (Fig. 4 C, lane 4). However, the coexpression of human IRSp53$^{R11E/Q23E}$ or IRSp53^{K143E} with GFP-Rac1^{G12V} and mIRS-KD had little effect on mIRS-KD's function in the Rac1^{G12V}-dependent formation of lamellipodia (Fig. 4 C, lanes 5 and 6). Therefore, the interaction between IRSp53 and active Rac1 is important for lamellipodia to form. These results suggest that IRSp53 is one of the targets of Rac1^{G12V} in the Rac1^{G12V}-dependent development of lamellipodia. However, overexpression of Kank and Kank^{S167A} had little effect on the formation of filopodia induced by a constitutively active form of cdc42, cdc42^{G12V} (Fig. 5, lanes 3 and 4), which may imply that Kank was not involved in the cdc42^{G12V}-mediated formation of microspikes.

Depletion of Kank promotes lamellipodial development

Based on the finding that Kank bound to IRSp53 and inhibited active Rac1-mediated lamellipodial development, as well as reports of IRSp53 as a downstream target of Rac1 (Miki et al., 2000; Miki and Takenawa, 2002), we examined the effect of KD of Kank on the formation of lamellipodia (Fig. 6). NIH3T3 cells were transfected with a Kank KD vector that targeted mouse *Kank* transcripts, a control KD vector, and an mIRS-KD as indicated in Fig. 6. Because we used plasmids containing a *neo-gfp* fusion gene in this assay, transfected cells can be stained with an anti-GFP antibody against GFP or can be detected with GFP fluorophore. The cells were cultured for 48 h

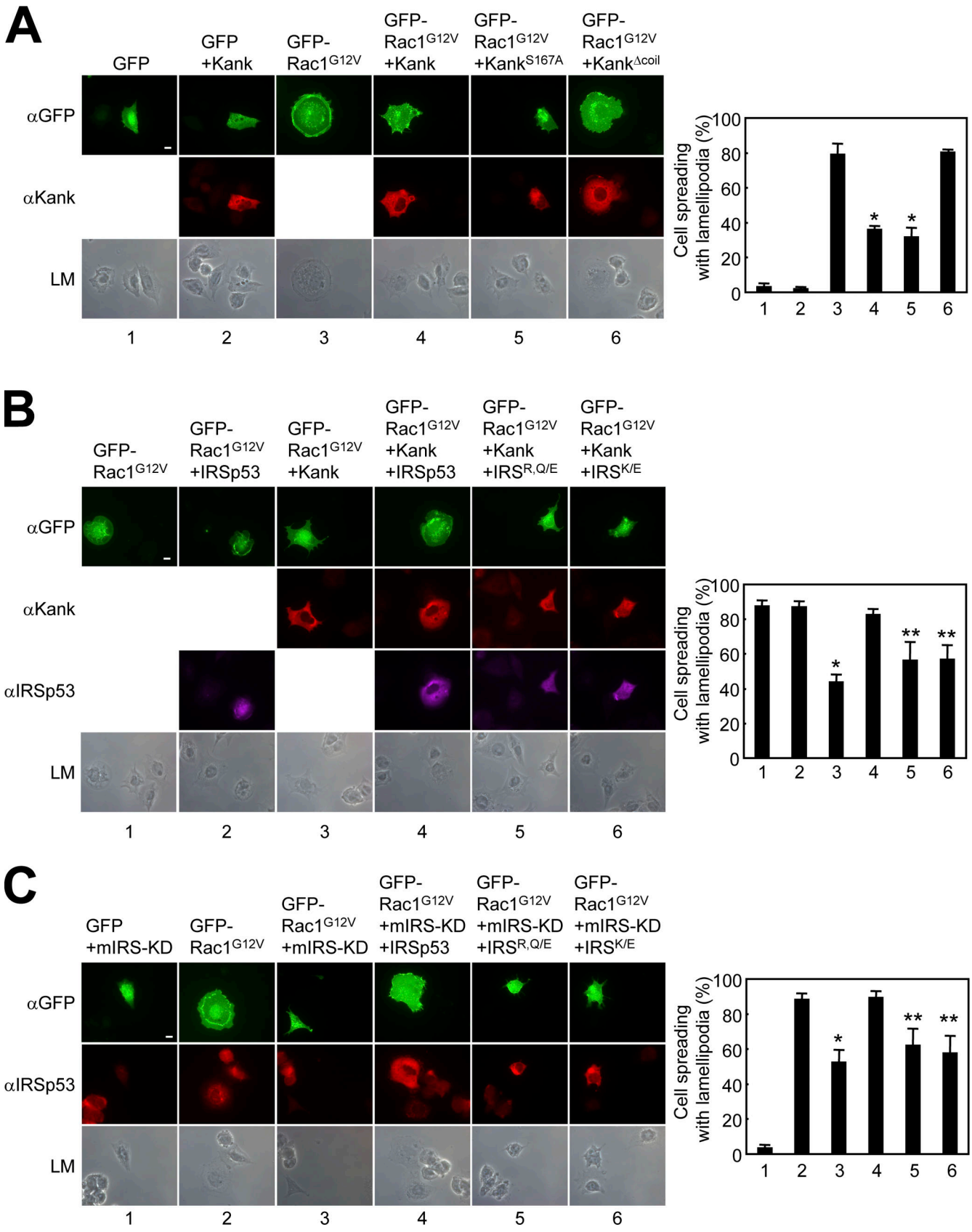

Figure 4. **Expression of Kank inhibits lamellipodial development mediated by active Rac1 through IRSp53.** (A) Effect of the expression of Kank on active Rac1-induced formation of lamellipodia. NIH3T3 cells were transfected as indicated, treated as described in Materials and methods, and stained for GFP (green) and Kank or its mutants (red). The number of cells spreading with lamellipodia is shown on the right as a percentage of the total number of transfected cells. *, $P < 0.001$ compared with lane 3. (B) Overexpression of IRSp53 abolished the effect of Kank on $Rac1^{G12V}$-dependent lamellipodial

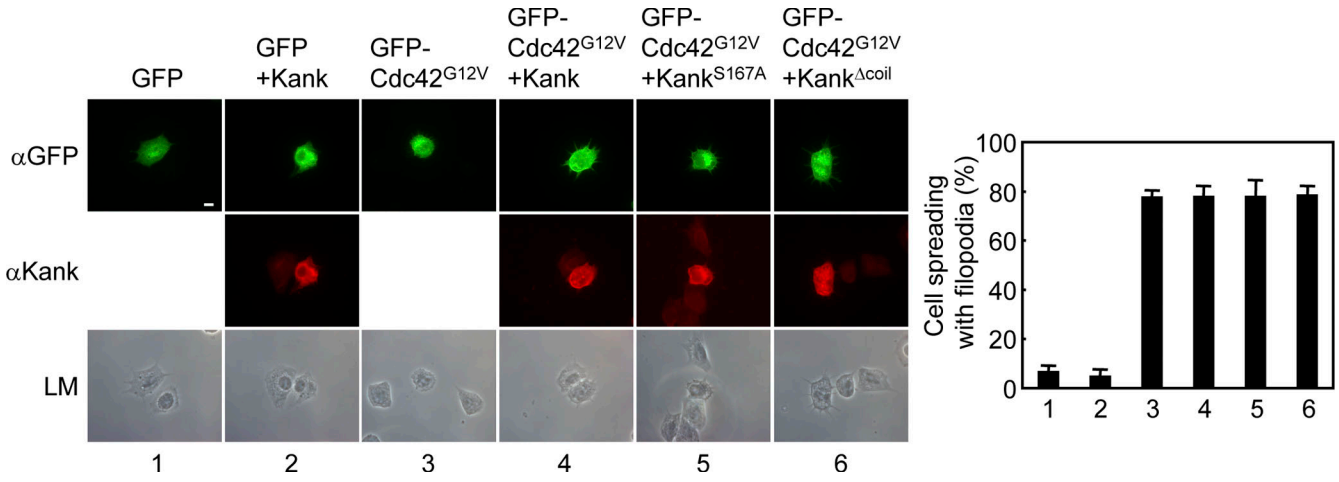

Figure 5. **Kank has no effect on active cdc42-dependent filopodial development.** The effect of Kank expression on active cdc42-dependent formation of filopodia was examined. NIH3T3 cells were transfected as indicated, treated as described in Materials and methods, and stained for GFP (green) and Kank or its mutants (red). The number of cells spreading with filopodia is shown on the right as a percentage of the total number of transfected cells. The results are shown as the mean ± SD for triplicate experiments in which ~100 cells per experiment were counted. LM, phase-contrast light microscopic image. Bar, 10 μm.

after transfection and fixed and stained with anti-GFP antibody (Fig. 6 B; green) or with phalloidin (Fig. 6 B; red). Transfection of a KD vector (Kank-KD) effectively suppressed the expression of Kank protein by ~80% with respect to control-KD (Fig. 6 A, lanes 2 and 3), and mIRS-KD suppressed the expression of mIRS protein by ~100% with respect to control-KD (Fig. 6 A, lanes 3 and 4). A careful observation of cell morphology revealed that silencing of Kank resulted in the formation of lamellipodia (Fig. 6 B, lane 2). However, the silencing of both Kank and IRSp53 simultaneously had little effect (Fig. 6 B, lane 3). These findings support the idea that Kank inhibits lamellipodia from forming by interrupting the interaction between active Rac1 and IRSp53.

Kank inhibits insulin-induced membrane ruffling

Lamellipodia and filopodia are formed at the leading edge in migrating cells in response to growth factors, chemokines, and extracellular matrix molecules (Ridley et al., 2003). Insulin acts as a growth factor, and insulin-stimulated KB cells, a strain derived from human epidermoid carcinoma, show membrane ruffling and Rac1 activation (Nishiyama et al., 1994). Overexpression of Kank inhibited active Rac1-dependent lamellipodial development (Fig. 5), and KD of Kank enhanced the formation of lamellipodia (Fig. 6). We then investigated whether Kank can inhibit insulin-induced membrane ruffling (Fig. 7). Whereas serum-starved NIH3T3 cells without treatment showed little membrane ruffling (Fig. 7, lane 1), insulin-stimulated cells exhibited extensive membrane ruffling (Fig. 7, lane 2). When Kank was overexpressed, the number of cells with membrane ruffling was significantly decreased (Fig. 7, lane 3). However, the effect of overexpression of Kank was not observed when IRSp53 was coexpressed (Fig. 7, lane 5). This result suggests that IRSp53 abrogates the inhibitory effect of Kank on insulin-induced membrane ruffling and, thus, that Kank inhibits insulin-induced membrane ruffling through IRSp53.

Kank inhibits integrin-mediated cell spreading through IRSp53

Integrins are major adhesion receptors in vertebrates and play major roles in cell adhesion and in a variety of intracellular signaling pathways (Hynes, 2002). The Rho family of small GTPases such as Rac1 and cdc42 are involved in integrin-mediated cell spreading (Clark et al., 1998; Price et al., 1998; Katoh and Negishi, 2003; Choi et al., 2005). As Kank interrupted the interaction between active Rac1 and IRSp53 (Fig. 3), we hypothesized that it might inhibit integrin-mediated cell spreading. To investigate the role of Kank downstream of integrin signaling, NIH3T3 cells were transfected, seeded on fibronectin-coated glass substrata, fixed, and stained with phalloidin (Fig. 8 A). The cells adhered rapidly to the substrata and completed spreading in 30 min, showing a normal shape (Fig. 8 A, lane 1). However, the expression of the wild-type Kank radically changed cell shape and markedly inhibited cell spreading (Fig. 8 A, lane 2). Notably, this change was not caused by apoptosis because

formation. NIH3T3 cells were transfected as indicated, treated as described in Materials and methods, and stained for Kank (red) and human IRSp53 or its mutants (purple). GFP is shown in green. The number of cells spreading with lamellipodia is shown as in A. *, $P < 0.001$ compared with lane 1; **, $P < 0.01$ compared with lane 1 or 4. $IRS^{R,Q/E}$, human IRSp53 with arginine replaced by glutamic acid at position 11 and glutamine replaced by glutamic acid at position 23; $IRS^{K/E}$, human IRSp53 with lysine replaced by glutamic acid at position 143. (C) KD of mIRS (mIRS-KD) decreased $Rac1^{G12V}$-dependent lamellipodial formation. NIH3T3 cells were transfected as indicated, treated as described in Materials and methods, and stained for GFP (green) and mIRS (endogenous) with human IRSp53 (expressing transiently) or its mutants (red). The number of cells spreading with lamellipodia is shown as in A. *, $P < 0.001$ compared with lane 2; **, $P < 0.01$ compared with lane 2 or 4. LM, phase-contrast light microscopic image. The results are shown as the mean ± SD for triplicate experiments in which ~100 cells per experiment were counted. Bars, 10 μm.

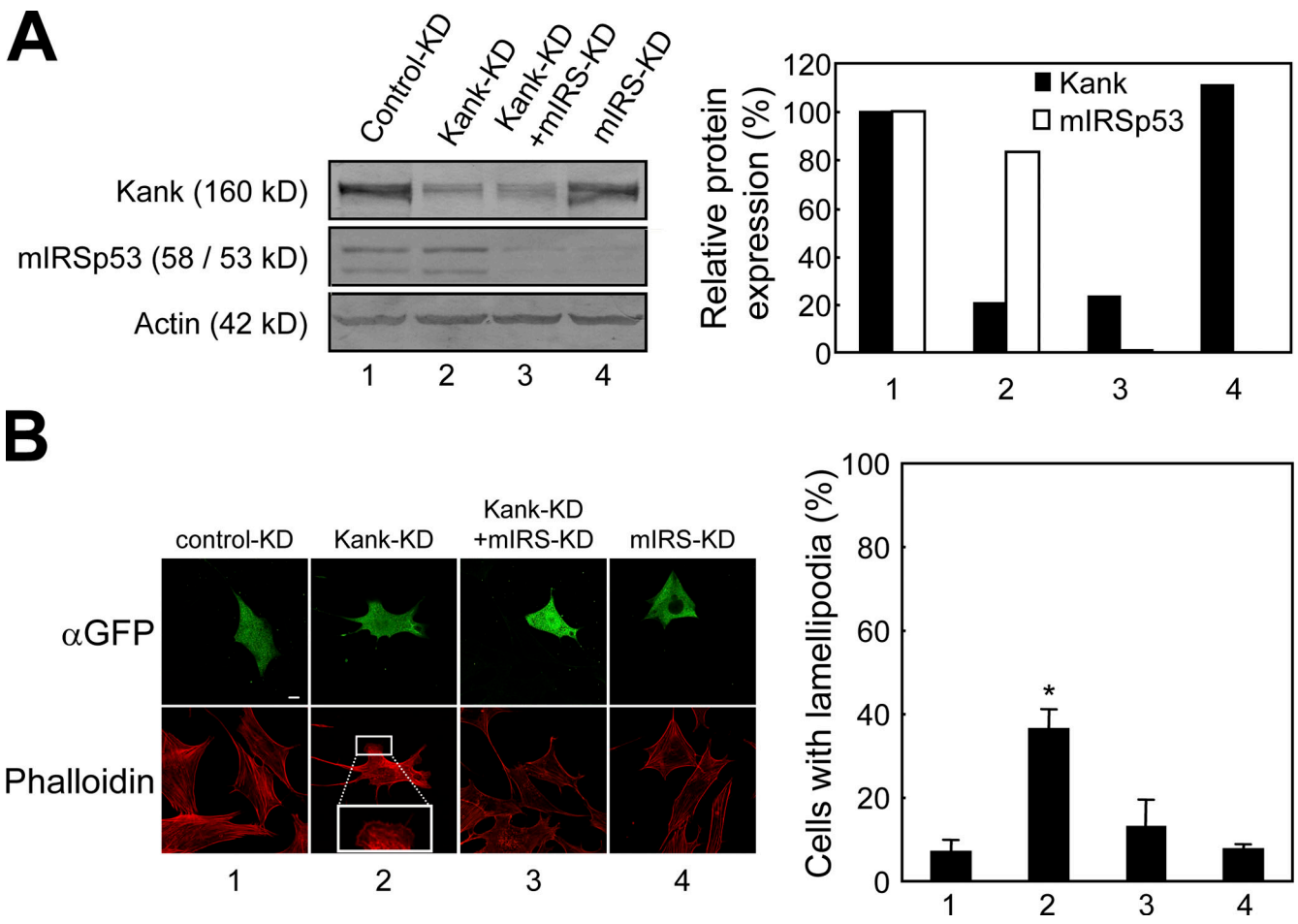

Figure 6. **Deletion of Kank significantly increases lamellipodial development through IRSp53.** (A) Relative expression of Kank and IRSp53 in NIH3T3 cells expressing RNAi. The levels of expression of Kank and mIRS relative to the amount of actin in the cell lysates were analyzed by Western blotting and quantified. (B) Confocal laser microscopic images of NIH3T3 cells transfected with Kank-KD and/or IRSp53-KD constructs. pSUPER.neo+gfp constructs were transfected, and the cells were fixed and stained with anti-GFP antibody (green) and phalloidin (red). Transfected cells were indicated as GFP-expressing cells, which were likely to show KD of the protein as indicated. Kank-KD–dependent lamellipodial extension was magnified in the bottom panel (lane 2). Quantification of lamellipodia in NIH3T3 cells expressing Kank-KD and/or IRSp53-KD is summarized in a graph. The results are shown as the mean ± SD for three independent experiments in which ~100 cells were counted in each experiment. *, $P < 0.001$ compared with lane 1. Bar, 10 μm.

nuclear staining of transfected cells with DAPI did not show any sign of apoptosis (unpublished data) and the cells were viable, as they could spread later (unpublished data). Kank$^{\Delta coil}$, which cannot bind to IRSp53, did not show any significant changes in cell shape or cell spreading (Fig. 8 A, lane 3). Kank^{S167A}, which cannot bind to 14-3-3, partially inhibited cell spreading (Fig. 8 A, lane 4). We obtained similar results using COS-7 and HeLa cells (unpublished data). In contrast, a control protein with the coiled-coil domain, kinectin^{coil}, did not affect the spreading of NIH3T3 cells (Fig. 8 A, lane 5). From these results, Kank inhibits cell spreading specifically through its coiled-coil domain.

To see how Kank inhibits cell spreading and whether this phenomenon depends on IRSp53, Kank was coexpressed with IRSp53 in NIH3T3 cells (Fig. 8 B). When Kank was coexpressed with wild-type IRSp53, cell spreading was enhanced compared with that when only Kank was expressed (Fig. 8 B, compare lane 2 with lane 3). Integrin activates Rac1 and cdc42 (Price et al., 1998; Hynes, 2002). We then examined whether the inhibitory effect of Kank on cell spreading depends on IRSp53–Rac1 signaling. Kank was coexpressed with IRSp53$^{R11E/Q23E}$ or IRSp53^{K143E} in NIH3T3 cells when the cells were spreading (Fig. 8 B, lanes 4 and 5). Surprisingly, the rates of spreading differed little between wild-type IRSp53, IRSp53$^{R11E/Q23E}$, and IRSp53^{K143E} when Kank was present (Fig. 8 B, lanes 3–5). Next, we investigated whether IRSp53 was involved in the spreading of NIH3T3 cells (Fig. 8 C). KD of mIRS resulted in the inhibition of cell spreading (Fig. 8 C, compare lane 1 with lane 3). In contrast, KD of mIRS with overexpression of the wild type or the mutants of human IRSp53 did not affect the spreading of NIH3T3 cells (Fig. 8 C, lanes 4–6). Furthermore, there was almost no change in cell spreading with or without KD of IRSp53 when Kank was overexpressed (Fig. S3, available at http://www.jcb.org/cgi/content/full/jcb.200805147/DC1).

We then investigated the effect of Kank and IRSp53 expression on cell morphology when NIH3T3 cells were spreading upon stimulation with fibronectin (Fig. S4, available at http://www.jcb.org/cgi/content/full/jcb.200805147/DC1). Cell shapes were classified according to those in the process of matrix-based cell spreading (Applewhite et al., 2007). Overexpression of Kank

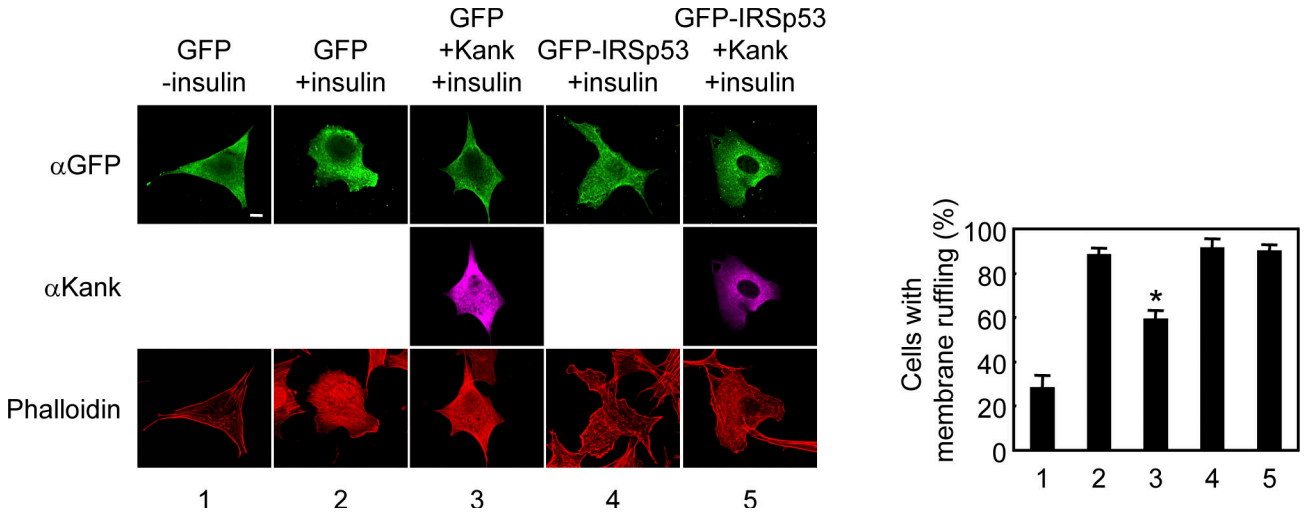

Figure 7. **Kank inhibits insulin-induced membrane ruffling.** The effect of Kank on insulin-induced membrane ruffling in NIH3T3 cells was examined. The cells were transfected and treated as described in Materials and methods. The images were obtained by confocal laser microscopy. The number of cells with membrane ruffling is shown on the right as a percentage of the total number of transfected cells. The results are shown as the mean ± SD for triplicate experiments in which 100 cells per experiment were counted. *, P < 0.001 compared with lane 2. Bar, 10 μm.

decreased the number of cells with the filopodial phenotype, whereas overexpression of IRSp53 increased the number of smooth-edged cells. Notably, coexpression of Kank and IRSp53 decreased the number of cells with the filopodial phenotype, whereas there was no increase in the number of the cells with the smooth-edged phenotype. These results suggest that Kank partially inhibits the spreading of NIH3T3 cells through IRSp53, although this phenomenon was not part of the Rac1–IRSp53 signaling pathway. The reason why IRSp53 partially recovers cell spreading inhibited by Kank might be that Kank inhibits the formation of both filopodial microspikes and lamellipodial sheets, whereas IRSp53 contributes only to lamellipodial sheets when the cells are spreading.

Kank inhibits IRSp53-mediated neurite outgrowth in N1E115 cells

Ectopic expression of IRSp53 in mouse neuroblastoma N1E115 cells induces neurite outgrowth (Govind et al., 2001; Miki and Takenawa, 2002), with Rac1 and cdc42 acting as positive regulators and Rho inhibiting the process (Kozma et al., 1995, 1997; Luo, 2000). To assess whether Kank is also involved in IRSp53-mediated neurite outgrowth, N1E115 cells were transfected with GFP-tagged IRSp53 to reproduce the morphological changes described previously (Govind et al., 2001). Overexpression of GFP-Kank inhibited neurite outgrowth under serum starvation (Fig. 9 A). The cells transfected with GFP-IRSp53 showed vigorous neuritic development in the presence or absence of serum (Fig. 9 B, second row). There were no round or adherent neurites when the cells were not transfected in the presence of serum. When Kank was coexpressed with GFP-IRSp53, the cells showed a phenotype similar to that seen with GFP alone (Fig. 9 B, bottom, Serum [+]). The quantitative analysis showed that Kank significantly reduced the extent of the IRSp53-induced outgrowth of neurites both in the presence (from 40 to 14%) and in the absence (from 85 to 25%) of serum (Fig. 9 B, graph). These findings demonstrate that Kank is involved in the IRSp53-mediated formation of neurites.

Discussion

In this study, we demonstrated that Kank plays a major role in the negative regulation of lamellipodial development in fibroblasts. The regulation is likely to be mediated by interaction with IRSp53 in ruffled areas of the cell. This binding seems to be constitutive because it was not affected by stimulation with a growth factor like PDGF or EGF (unpublished data). IRSp53 is a multidomain scaffolding protein (Govind et al., 2001; Krugmann et al., 2001; Soltau et al., 2002, 2004; Funato et al., 2004; Choi et al., 2005; Connolly et al., 2005; Hori et al., 2005) and a downstream target of Rac1 and links WAVE2 to Rac1 (Miki et al., 2000; Miki and Takenawa, 2002), which plays an important role in the reorganization of the actin cytoskeleton.

Kank contains two important domains, the coiled-coil and ankyrin repeat domains, both of which have been described in several structural proteins as well as in proteins involved in an array of cellular functions (Sedgwick and Smerdon, 1999; Burkhard et al., 2001). We showed in this study that the coiled-coil domain of Kank is necessary for binding with IRSp53 and the negative regulation of cell spreading and lamellipodial development induced by constitutively active Rac1 (Fig. 4).

Although active Rac1- or active cdc42-dependent actin polymerization has been described for the regulation of WASP and WAVE proteins (Bompard and Caron, 2004) and the regulation of Rac1 activity through three major classes of regulators, GTPase-activating proteins, guanine nucleotide exchange factors, and GDP dissociation inhibitors, has been identified, albeit with little understanding of the signaling pathways that modulate their activity (Burridge and Wennerberg, 2004), Kank does not possess any of these classical regulatory functions in Rac1 activation. This raises the possibility that Kank functions via other proteins also.

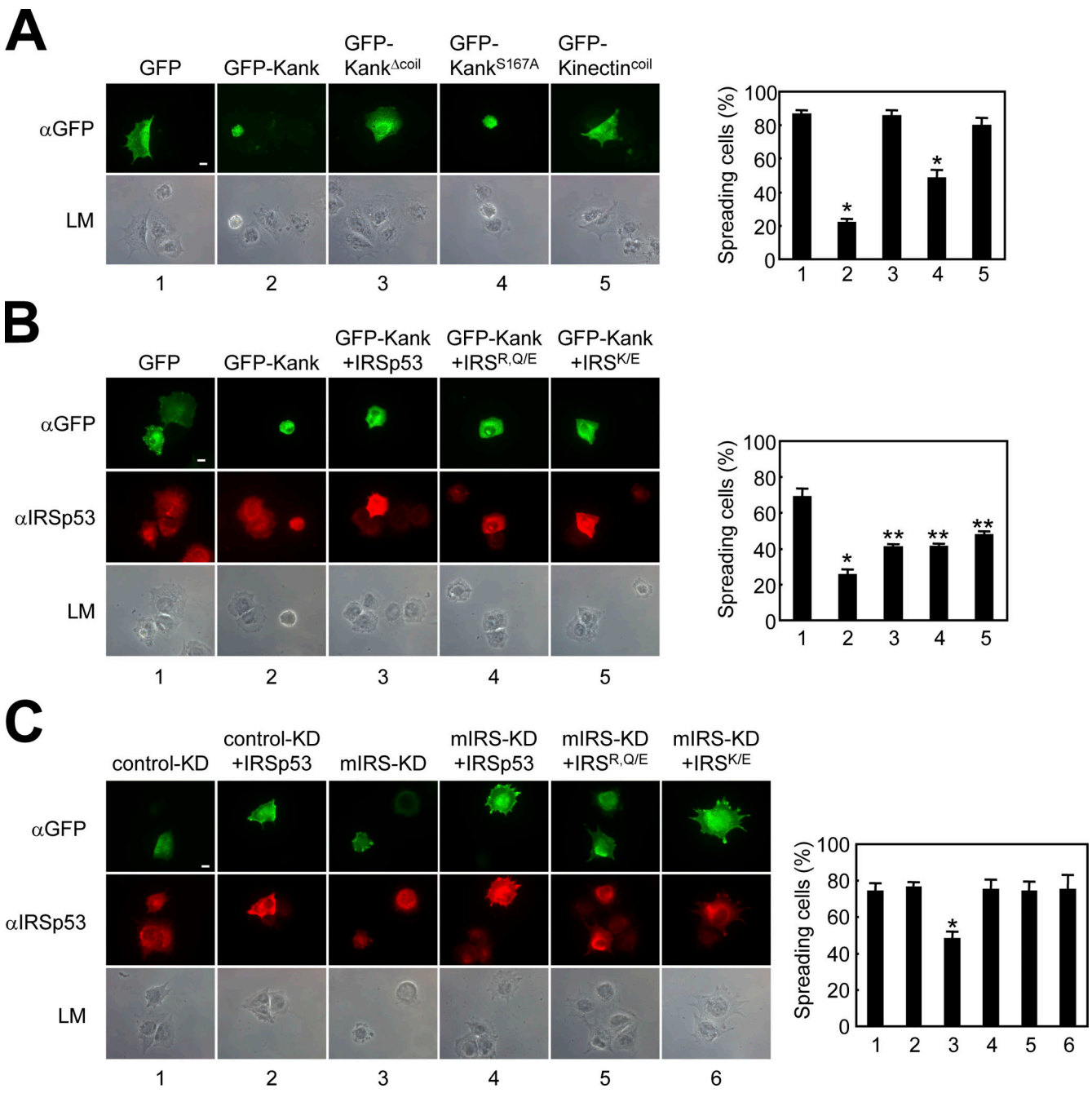

Figure 8. **Kank inhibits integrin-dependent cell spreading through IRSp53.** (A) Effect of Kank expression on cell spreading. NIH3T3 cells were transfected as indicated and treated as described in Materials and methods. The cells were then stained for GFP (green). The number of spreading cells is shown on the right as a percentage of the total number of transfected cells. *, $P < 0.001$ compared with lane 1. (B) Overexpression of IRSp53 partially abolished the effect of Kank on the spreading of NIH3T3 cells. The cells were transfected as indicated and treated as described in Materials and methods. The cells were stained for GFP (green) and IRSp53 or its mutants (red). The number of spreading cells was counted as in A. *, $P < 0.001$ compared with lane 1; **, $P < 0.001$ compared with lane 1 or 2. (C) Integrin-dependent cell spreading was mediated by IRSp53 in NIH3T3 cells. pSUPER.neo+gfp constructs were transfected with or without IRSp53 or its mutants as indicated. The cells were treated as described in Materials and methods and were stained for GFP (green) and IRSp53 or its mutants (red). The number of spreading cells was counted as in A. *, $P < 0.001$ compared with lane 1. mIRS-KD, IRS$^{R,Q/E}$, and IRS$^{K/E}$ are described in Fig. 4 (B and C). LM, phase-contrast light microscopic image. The results are shown as the mean ± SD for triplicate experiments in which ~100 cells per experiment were counted. Bars, 10 µm.

IRSp53 makes a complex with Eps8 and activates Rac1, which is important to cancer cell motility and invasion (Funato et al., 2004). Active cdc42 binds to the complex of IRSp53 and Eps8 and controls its cellular distribution, thereby contributing to the generation of actin bundles and promoting filopodial protrusions (Disanza et al., 2006). Eps8 was shown to form a complex with Abi-1, Sos-1, E3B1, and PI3-K, which activate Rac1 and transduce signals from Ras to Rac1 (Biesova et al., 1997; Scita et al., 1999, 2001; Innocenti et al., 2003). Tiam1, another Rac1 activator, also binds to IRSp53, leading to increased activation of Rac1 and enhanced binding of IRSp53 to both active Rac1 and WAVE2. Tiam1 promotes the

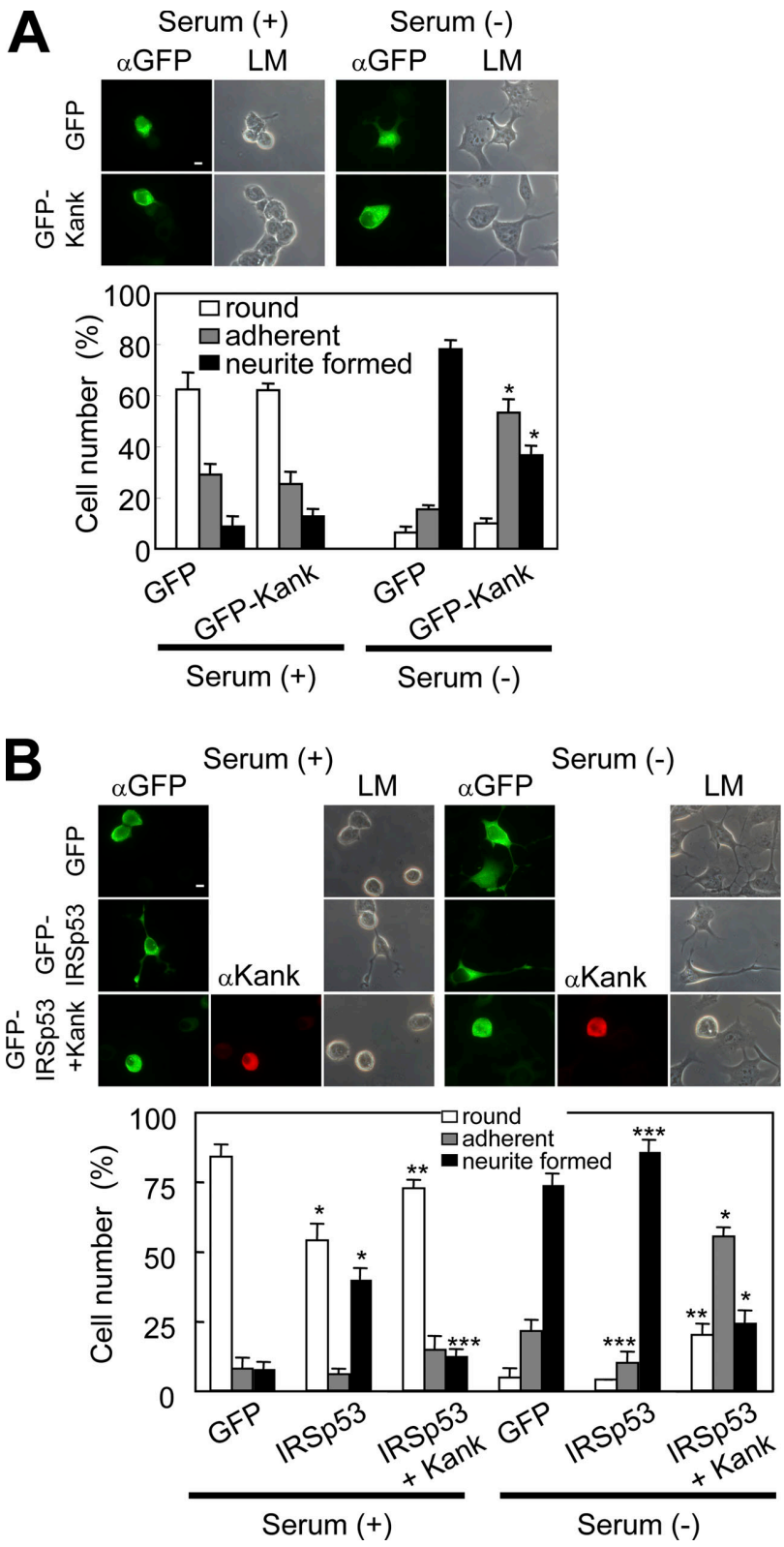

Figure 9. **Kank inhibits IRSp53-mediated neurite outgrowth in N1E115 cells.** (A) Suppression of neurite outgrowth by Kank in N1E115 cells. Fluorescence images were obtained for N1E115 cells expressing GFP alone or GFP-tagged Kank in the presence (left) or absence (right) of serum. The quantification of different phenotypes of N1E115 cells is summarized in a graph. *, $P < 0.001$ compared with GFP-expressing cells with the same morphology. (B) Suppression of IRSp53-mediated neurite outgrowth by Kank in N1E115 cells. Fluorescence images were obtained for N1E115 cells expressing GFP alone, GFP-tagged IRSp53 (IRSp53), or GFP-IRSp53 with coexpression of Kank (IRSp53 + Kank). The effect of the transient expression of GFP alone (top), GFP-IRSp53 (middle), or GFP-IRSp53 with Kank (bottom) in N1E115 cells in the presence (left) or absence (right) of serum. The quantification of different phenotypes of N1E115 cells is summarized in a graph. *, $P < 0.001$; **, $P < 0.01$; ***, $P < 0.05$ compared with GFP-expressing cells with the same morphology. LM, phase-contrast light microscopic image. The results are shown as the mean ± SD for three independent experiments in which ~100 transfected cells were counted. Bars, 10 μm.

localization of IRSp53 to Rac1-induced lamellipodia rather than cdc42-induced filopodia (Connolly et al., 2005). Similarly, Kank specifically inhibits the binding between IRSp53 and $Rac1^{G12V}$ rather than that between IRSp53 and $cdc42^{G12V}$ (Fig. 3, A and B), which is consistent with the finding that the coexpression of Kank with active Rac1 or active cdc42 in NIH3T3 cells showed marked differences: the formation of lamellipodia induced by active Rac1 was inhibited (Fig. 4), whereas microspikes or filopodia generated by active cdc42 showed some but not great alteration (Fig. 5). Because the IMD/RCB domain of IRSp53 overlaps with the Kank binding domain, Kank might disrupt the association of active Rac1 to

IRSp53. In contrast, the cdc42-binding domain of IRSp53 is located far from the Kank binding domain. This may be why Kank weakly inhibits cdc42-IRSp53 association. KD of Kank by RNAi in NIH3T3 cells revealed that depletion of Kank resulted in an increase in lamellipodia, whereas KD of both Kank and IRSp53 resulted in normal or unaltered cell shapes (Fig. 6 B). Moreover, Kank inhibited insulin-induced membrane ruffling, and coexpression of Kank with IRSp53 abrogated this inhibitory effect (Fig. 7). This suggests that Kank inhibits the IRSp53-dependent formation of lamellipodia. However, Kank inhibited integrin-dependent cell spreading through IRSp53, but this was not caused by Rac1 (Fig. 8, B and C). Kank also inhibited IRSp53-dependent neurite outgrowth in N1E115 (Fig. 9). Kank binds to the IMD/RCB domain of IRSp53, and it has been shown that this domain binds not only to active Rac1 but also to actin and lipids (Miki et al., 2000; Yamagishi et al., 2004; Millard et al., 2005; Suetsugu et al., 2006b). The IMD/RCB domain was also shown to have actin-bundling activity (Millard et al., 2005), although this activity may only be seen under nonphysiological conditions such as at a low ionic strength (Lee et al., 2007; Mattila et al., 2007). Consistent with this, we also found that actin was present in a complex immunoprecipitated with an anti-IRSp53 antibody in HEK293 cells (Fig. S5, available at http://www.jcb.org/cgi/content/full/jcb.200805147/DC1). Expression of Kank is likely to inhibit the association of IRSp53 with actin, which implies that Kank negatively regulates the association of IRSp53 with actin. This might be why Kank inhibits the spreading of NIH3T3 cells and the outgrowth of neurites in N1E115 cells through the binding of IRSp53.

Kank regulates RhoA activity through its 14-3-3 binding motif inside the coiled-coil domain (Kakinuma et al., 2008). Kank inhibited Rac1–IRSp53 signaling, which is mediated by the coiled-coil domain (Fig. 4). However, the formation of lamellipodia induced by active Rac1 was inhibited by both Kank and Kank^{S167A}, which cannot bind to 14-3-3 and was ineffective against active RhoA (Fig. 4 A, lanes 4 and 5). From this finding, the effect of Kank on active Rac1-induced lamellipodial development can be separated from the effect of the binding of 14-3-3 to Kank. In contrast, overexpression of Kank^{S167A} was relatively ineffective compared with the effect of wild-type Kank on integrin-dependent cell spreading (Fig. 8 A, compare lane 2 with lane 4). A deletion mutant, Kank$^{\Delta coil}$, was not completely effective against integrin-dependent cell spreading (Fig. 8 A, lane 3); Kank may affect the integrin-dependent cell spreading mediated by both IRSp53 and 14-3-3 or more likely through the Kank coiled-coil domain.

Although there are orthologues of Kank in different species, in which the coiled-coil domain along with the ankyrin repeat domain are conserved, only VAB-19 of *C. elegans* has been studied and was shown to be a component of the epidermal attachment structure and to interact with actin (Ding et al., 2003). This further strengthens our finding that Kank functions through the coiled-coil domain in the regulation of actin remodeling. This function of Kank in the reorganization of the actin cytoskeleton may be conserved in other orthologues as well. Further studies are needed to explore other potential roles of Kank or the Kank–IRSp53 complex in response to external stimuli, which may contribute to our understanding of the cell signaling mechanisms in renal cell carcinoma.

Materials and methods

Expression vectors and antibodies

Cytomegalovirus-driven Flag-tagged constructs (Agilent Technologies), GFP-tagged constructs (BD), the vector pcDNA-3.1 (Invitrogen), the hEF1-α–driven expression vector pEF1/myc-His (Invitrogen), and a bacterial expression vector for GST, pGEX-5x-1(GE Healthcare), were generated by recombinant PCR. Full-length human IRSp53 cDNA was obtained by RT-PCR. Kank mutants and human IRSp53 mutants were made by PCR-mediated recombination. The coiled-coil domain of kinectin (kinectin^{coil}) was obtained by RT-PCR and used as a control (Vignal et al., 2001). All of the constructs were verified by sequencing. Polyclonal and monoclonal antibodies against Kank were described previously (Sarkar et al., 2002; Roy et al., 2005). The polyclonal antibody against mouse Kank recognizes a peptide spanning amino acids 861–975 (Kakinuma et al., 2008). The polyclonal antibody against IRSp53 was a gift from M. Yamada (National Research Institute for Child Health and Development, Tokyo, Japan; Okamura-Oho et al., 1999) or was generated in a rabbit using the C-terminal part of the protein (163 residues long, amino acids 358–521) fused to GST as an antigen and was prepared by affinity purification. A monoclonal antibody against autofluorescent proteins (MP Biomedicals), a rabbit antiserum against GFP (Invitrogen), a polyclonal antibody against GFP (Clontech Laboratories, Inc.), a monoclonal antibody against cdc42 protein, a polyclonal antibody against EGF receptor (Santa Cruz Biotechnology, Inc.), a monoclonal antibody against Rac1 (Transduction Laboratories), a goat polyclonal antibody against WAVE2 (Santa Cruz Biotechnology, Inc.), and monoclonal antibodies against Flag, GFP, β-actin, and β-tubulin (Sigma-Aldrich) were purchased.

Cell culture, immunoprecipitation, and immunoblotting

HEK293 cells stably expressing Rac1^{G12V} were constructed with the pcDNA4/TO expression vector (Invitrogen). NIH3T3, HeLa, N1E115 (a gift from Y. Kanaho, Tsukuba University, Ibaraki, Japan), HEK293 (a gift from M. Noguchi, Hokkaido University, Hokkaido, Japan), and HEK293T cells were cultured in DME supplemented with 10% FBS. VMRC-RCW cells were cultured in MEM with 10% FBS. Transfection was performed using Lipofectamine 2000 (Invitrogen) and Effectine (QIAGEN) according to the manufacturers' instructions. After 30 h, cells were harvested, washed with ice-cold PBS, and lysed for 15 min on ice in buffer A (50 mM Tris-HCl, pH 7.5, 140 mM NaCl, 10% glycerol, 1% Nonidet P-40, 100 mM NaF, 200 mM Na_3VO_4, 1 mM PMSF, 10 μg/ml leupeptin, 10 μg/ml aprotinin, and 10 μg/ml chymotrypsin). The cell lysates were clarified by centrifugation, and the proteins were immunoprecipitated, washed in the lysis buffer, and boiled in an SDS-PAGE loading buffer. Proteins were separated by SDS-PAGE, transferred to polyvinylidene difluoride membranes (Immobilon; Millipore), and detected with respective antibodies. Signals were enhanced with secondary antibody against AP (Sigma-Aldrich) or HRP (GE Healthcare) and developed with nitroblue tetrazolium/5-bromo-4-chloro-3-indolyl phosphate (Sigma-Aldrich) or ECL (GE Healthcare). The intensity of the bands was quantified by ImageJ software (National Institutes of Health).

Immunocytochemistry

The cells on coverslips were fixed with 3.7% formaldehyde-PBS for 30 min and permeabilized with 0.25% Triton X-100–PBS for 10 min. The cells were subsequently incubated with the primary and secondary antibodies. The secondary antibodies used were Alexa Fluor 594–conjugated goat anti–mouse and anti–rabbit IgG (Invitrogen), Alexa Fluor 488–conjugated goat anti–mouse and anti–rabbit IgG (Invitrogen), RITC-conjugated donkey anti–goat IgG (Santa Cruz Biotechnology, Inc.), and Cy5-conjugated goat anti–rabbit IgG (Millipore). Filamentous actin (F-actin) was stained with TRITC-conjugated phalloidin (Sigma-Aldrich). Images of cells after they were mounted were acquired at room temperature in 80% (wt/vol) glycerol in PBS using AxioVision 3.1 software (Carl Zeiss, Inc.) and a fluorescence microscope (Axioskop 2 Plus; Carl Zeiss, Inc.) with a Plan-NEOFLUAR 40× NA 0.75 objective (Carl Zeiss, Inc.) and a color camera (AxioCam HRc; Carl Zeiss, Inc.). Confocal laser microscopy was performed using a laser-scanning confocal microscope (Axiovert 200M; Carl Zeiss, Inc.) with LSM510 META software (Carl Zeiss, Inc.). Optical thickness was set at 1.0 μm in Z height with a Plan-Apochromat 63× NA

1.4 oil immersion objective (Carl Zeiss, Inc.). All images were prepared with Photoshop 7.0 (Adobe).

Formation of lamellipodia and filopodia
NIH3T3 cells were transfected as indicated and incubated for 24 h (for overexpression) or 48 h (for KD). The cells were then trypsinized and seeded on 10 µg/ml fibronectin-coated coverslips. After incubation overnight, they were subjected to immunostaining as described in Immunocytochemistry. The cells with lamellipodia were those with broad ruffles, whereas the cells with filopodia were those with >15 microspikes in phase-contrast images.

Insulin-induced membrane ruffling
NIH3T3 cells were transfected as indicated. After 4 h, the cells were trypsinized and seeded onto fibronectin-coated coverslips. When they had adhered to coverslips completely, the cells were serum starved by culturing them in 0.5% FBS-DME for 2 d. Then, the cells were treated with 10 µg/ml insulin for 6 h. The cells with membrane ruffling were counted from phase-contrast images and the images for F-actin (phalloidin) staining.

Cell spreading assay
Integrin stimulation was performed as described previously (Katoh and Negishi, 2003). In brief, cells were transfected as indicated, incubated with trypsin, and suspended in a serum-free medium containing 1 mg/ml of trypsin inhibitor (from soybeans; Sigma-Aldrich). After 1 h, the cells were transferred onto fibronectin-coated coverslips and cultured for 30 min. The number of spreading cells was counted for the cells that were completely adhered and examined by phase-contrast microscopy. The classification of spreading cell morphology was performed as described previously (Applewhite et al., 2007). In brief, the cells were transfected as indicated and after 24 h were trypsinized and seeded on fibronectin-coated coverslips. The cells were incubated for 30–40 min to allow them to attach and spread. They were immunostained as described in Immunocytochemistry. Morphological typing was performed based on F-actin (phalloidin) staining and phase-contrast images.

Neurite outgrowth in N1E115 cells
The N1E115 cells were seeded on 10 µg/ml laminin-coated coverslips and cultured overnight. The next day, they were transfected with the respective expression vectors in the presence of serum. After 16 h, the cells were serum starved for another 12 h, immunostained as described in Immunocytochemistry, and analyzed as described previously (Miki and Takenawa, 2002; Yamazaki et al., 2002). In brief, cells with neurites were defined as the cells possessing at least one neurite two times longer than the diameter of the cell body from phase-contrast images.

Subcellular fractionation
HeLa cells suspended in hypotonic buffer (10 mM Tris-HCl, pH 7.5, 1 mM EGTA, 1 mM $MgCl_2$, 50 mM NaF, 1 mM Na_3VO_4, and a protease inhibitor cocktail; Sigma-Aldrich) were homogenized by 10 passages through a 22-gauge needle. The samples were then centrifuged at 4,300 *g* for 10 min, and the supernatants were again centrifuged at 50,000 *g* for 1 h to separate the cytosolic and membrane fractions. The membrane fraction was washed three times with the hypotonic buffer and dissolved in buffer A with 1% SDS. The protein in the cytosolic and membrane fractions was quantified using a DC Protein Assay kit (Bio-Rad Laboratories). Each fraction was mixed with SDS sample buffer, and aliquots of the samples containing 30 µg of protein were analyzed by Western blotting.

siRNA
An H1 promoter–based mammalian expression vector, pSUPER.neo, or pSUPER.neo+gfp, which coexpresses siRNA and a *neo-gfp* fusion gene (OligoEngine), was used for the expression of siRNA in mouse NIH3T3 fibroblasts. A 19-nucleotide sequence corresponding to nucleotides 609–627 (5′-GAGGCGAAAGCCATCTGTG-3′) of the mouse cDNA clone A530060J16 (available from GenBank/EMBL/DDBJ under accession no. AK041011.1) was used as the Kank RNAi (Kank-KD) vector. A control vector was constructed using a 19-nucleotide sequence (5′-ACTAGACGAAGCGGTACTG-3′) with no significant homology to any mammalian gene sequences and used as a nonsilencing control (control #2 in Suetsugu et al., 2006a). For KD of mIRS, we searched for candidate KD sequences by Sfold (http://sfold.wadsworth.org/), tested their efficiency using NIH3T3 cells (Fig. S2), and selected a 19-nucleotide sequence (#513) corresponding to nucleotides 513–531 (5′-GTAAGAACCCTCAGAAGTA-3′) of mIRS (available from GenBank/EMBL/DDBJ under accession no. AF390179). For transfection, after cells were grown to 80–90% confluency, they were detached with trypsin/EDTA, washed with PBS, suspended at ~10^6 cells/ml in PBS, and subjected to electroporation. Electroporation was performed with 18 µg of plasmid DNA using a Gene Pulser II System (Bio-Rad Laboratories) at 270 mV and 975-µF capacitance. Under these conditions, we estimated the transfection efficiency to be around 50–70% by comparing the level of expression of GFP in a parallel experiment. After electroporation, the cells were kept on ice for 5 min and transferred to plates with 10 ml of a complete medium. After 36 h, the cells were lysed in a lysis buffer for checking the expression of Kank protein. Kank esiRNA was prepared as described previously (Yang et al., 2002; Kittler et al., 2004). In brief, sense and antisense RNA was transcribed using a T7 promoter system (for both strands) supplied in the MEGAscript kit (Applied Biosystems). After annealing the sense and antisense strands, RNA was treated with ShortCut RNase III (New England Biolabs, Inc.) and purified with Sepharose Q (GE Healthcare). Kank esiRNA and control esiRNA containing the *Xenopus laevis* elongation factor gene (from the MEGAscript kit) were transfected with Lipofectamine 2000 in HEK293 cells stably expressing $Rac1^{G12V}$.

In vitro binding assay
1 µg His-$Rac1^{G12V}$ or His-$cdc42^{G12V}$, which was produced in bacteria and purified with an Ni column, was added with 2 µg of control GST or GST-IRSp53(N) and 10 µg MBP or 1, 3, or 10 µg MBP-$Kank^{coil}$ as competitor in binding buffer A. After these mixtures were rotated for 1 h at 4°C, glutathione–Sepharose 4B (GE Healthcare) was added to recover the protein complexes, and rotation was continued for 1 h at 4°C. The complexes were washed four times with the binding buffer, boiled for 5 min in an SDS-PAGE loading buffer, and subjected to 5–20% SDS-PAGE, Coomassie blue staining, and Western blot analysis using anti-Rac1 or anti-cdc42 antibodies to detect the respective proteins. The intensity of the bands was quantified by CS Analyzer (ATTO Corp.).

Online supplemental material
Fig. S1 shows IRSp53 mutants that bind to $Kank^{coil}$ but not to $Rac1^{G12V}$. Fig. S2 shows the candidate sequences for IRSp53 KD. Fig. S3 shows that KD of IRSp53 does not affect fibronectin-stimulated cell spreading when Kank is overexpressed. Fig. S4 shows that Kank inhibits the formation of the cells with filopodial- and IRSp53-induced smooth-edged phenotypes when cells are spreading. Fig. S5 shows that overexpression of Kank inhibits the association of IRSp53 with actin. Online supplemental material is available at http://www.jcb.org/cgi/content/full/jcb.200805147/DC1.

We thank Professor T. Akiyama (the University of Tokyo, Tokyo, Japan) for advice and discussions, Dr. M. Yamada for the anti-IRSp53 serum, Professor M. Noguchi for HEK293 cells, Professor Y. Kanaho for N1E115 cells, and Professor R. Matsuoka and Dr. Y. Furutani (Tokyo Women's Medical University, Tokyo, Japan) for laser-scanning confocal microscopy.

This work was supported by the Special Coordination Fund for Promoting Science and Technology by the Ministry of Education, Culture, Sports, Science, and Technology of Japan and by a fund for promoting collaboration with small and medium enterprises from the National Institute of Advanced Industrial Science and Technology.

Submitted: 23 May 2008
Accepted: 22 December 2008

References

Applewhite, D.A., M. Barzik, S. Kojima, T.M. Svitkina, F.B. Gertler, and G.G. Borisy. 2007. Ena/VASP proteins have an anti-capping independent function in filopodia formation. *Mol. Biol. Cell*. 18:2579–2591.

Aspenström, P. 1999. Effectors for the Rho GTPases. *Curr. Opin. Cell Biol.* 11:95–102.

Biesova, Z., C. Piccoli, and W.T. Wong. 1997. Isolation and characterization of e3B1, an eps8 binding protein that regulates cell growth. *Oncogene*. 14:233–241.

Bompard, G., and E. Caron. 2004. Regulation of WASP/WAVE proteins: making a long story short. *J. Cell Biol.* 166:957–962.

Burbelo, P.D., D. Drechsel, and A. Hall. 1995. A conserved binding motif defines numerous candidate target proteins for both Cdc42 and Rac GTPases. *J. Biol. Chem.* 270:29071–29074.

Burkhard, P., J. Stetefeld, and S.V. Strelkov. 2001. Coiled coils: a highly versatile protein folding motif. *Trends Cell Biol.* 11:82–88.

Burridge, K., and K. Wennerberg. 2004. Rho and Rac take center stage. *Cell*. 116:167–179.

Choi, J., J. Ko, B. Racz, A. Burette, J.R. Lee, S. Kim, M. Na, H.W. Lee, K. Kim, R.J. Weinberg, and E. Kim. 2005. Regulation of dendritic spine morphogenesis by insulin receptor substrate 53, a downstream effector of Rac1 and Cdc42 small GTPases. *J. Neurosci.* 25:869–879.

Clark, E.A., W.G. King, J.S. Brugge, M. Symons, and R.O. Hynes. 1998. Integrin-mediated signals regulated by members of the rho family of GTPases. *J. Cell Biol.* 142:573–586.

Connolly, B.A., J. Rice, L.A. Feig, and R.J. Buchsbaum. 2005. Tiam1-IRSp53 complex formation directs specificity of rac-mediated actin cytoskeleton regulation. *Mol. Cell. Biol.* 25:4602–4614.

Ding, M., A. Goncharov, Y. Jin, and A.D. Chisholm. 2003. *C. elegans* ankyrin repeat protein VAB-19 is a component of epidermal attachment structures and is essential for epidermal morphogenesis. *Development*. 130:5791–5801.

Disanza, A., S. Mantoani, M. Hertzog, S. Gerboth, E. Frittoli, A. Steffen, K. Berhoerster, H.J. Kreienkamp, F. Milanesi, P.P. Di Fiore, et al. 2006. Regulation of cell shape by Cdc42 is mediated by the synergic actin-bundling activity of the Eps8-IRSp53 complex. *Nat. Cell Biol.* 8:1337–1347.

Eden, S., R. Rohatgi, A.V. Podtelejnikov, M. Mann, and M.W. Kirschner. 2002. Mechanism of regulation of WAVE1-induced actin nucleation by Rac1 and Nck. *Nature*. 418:790–793.

Etienne-Manneville, S., and A. Hall. 2002. Rho GTPases in cell biology. *Nature*. 420:629–635.

Funato, Y., T. Terabayashi, N. Suenaga, M. Seiki, T. Takenawa, and H. Miki. 2004. IRSp53/Eps8 complex is important for positive regulation of Rac and cancer cell motility/invasiveness. *Cancer Res.* 64:5237–5244.

Govind, S., R. Kozma, C. Monfries, L. Lim, and S. Ahmed. 2001. Cdc42Hs facilitates cytoskeletal reorganization and neurite outgrowth by localizing the 58-kD insulin receptor substrate to filamentous actin. *J. Cell Biol.* 152:579–594.

Hall, A. 1998. Rho GTPases and the actin cytoskeleton. *Science*. 279:509–514.

Higgs, H.N., and T.D. Pollard. 2000. Activation by Cdc42 and PIP_2 of Wiskott-Aldrich Syndrome protein (WASp) stimulates actin nucleation by Arp2/3 complex. *J. Cell Biol.* 150:1311–1320.

Hori, K., H. Yasuda, D. Konno, H. Maruoka, T. Tsumoto, and K. Sobue. 2005. NMDA receptor-dependent synaptic translocation of insulin receptor substrate p53 via protein kinase C signaling. *J. Neurosci.* 25:2670–2681.

Hynes, R.O. 2002. Integrins: bidirectional allosteric signaling machines. *Cell*. 110:673–687.

Innocenti, M., E. Frittoli, I. Ponzanelli, J.R. Falck, S.M. Brachmann, P.P. Di Fiore, and G. Scita. 2003. Phosphoinositide 3-kinase activates Rac by entering in a complex with Eps8, Abi1, and Sos-1. *J. Cell Biol.* 160:17–23.

Innocenti, M., A. Zucconi, A. Disanza, E. Frittoli, L.B. Areces, A. Steffen, T.E. Stradal, P.P. Di Fiore, M.F. Carlier, and G. Scita. 2004. Abi1 is essential for the formation and activation of a WAVE2 signalling complex. *Nat. Cell Biol.* 6:319–327.

Kakinuma, N., B.C. Roy, Y. Zhu, Y. Wang, and R. Kiyama. 2008. Kank regulates RhoA-dependent formation of actin stress fibers and cell migration via 14-3-3 in PI3K–Akt signaling. *J. Cell Biol.* 181:537–549.

Katoh, H., and M. Negishi. 2003. RhoG activates Rac1 by direct interaction with the Dock180-binding protein Elmo. *Nature*. 424:461–464.

Kittler, R., G. Putz, L. Pelletier, I. Poser, A.K. Heninger, D. Drechsel, S. Fischer, I. Konstantinova, B. Habermann, H. Grabner, et al. 2004. An endoribonuclease-prepared siRNA screen in human cells identifies genes essential for cell division. *Nature*. 432:1036–1040.

Kozma, R., S. Ahmed, A. Best, and L. Lim. 1995. The Ras related protein Cdc42Hs and bradykinin promote formation of peripheral actin microspikes and filopodia in Swiss 3T3 fibroblasts. *Mol. Cell. Biol.* 15:1942–1952.

Kozma, R., S. Ahmed, A. Best, and L. Lim. 1996. The GTPase-activating protein n-chimaerin cooperates with Rac1 and Cdc42Hs to induce the formation of lamellipodia and filopodia. *Mol. Cell. Biol.* 16:5069–5080.

Kozma, R., S. Sarner, S. Ahmed, and L. Lim. 1997. Rho family GTPases and neuronal growth cone remodelling: relationship between increased complexity induced by Cdc42Hs, Rac1 and acetylcholine and collapse induced by RhoA and lysophosphatidic acid. *Mol. Cell. Biol.* 17:1201–1211.

Krugmann, S., I. Jordens, K. Gevaert, M. Driessens, J. Vandekerckhove, and A. Hall. 2001. Cdc42 induces filopodia by promoting the formation of an IRSp53:Mena complex. *Curr. Biol.* 11:1645–1655.

Lee, S.H., F. Kerff, D. Chereau, F. Ferron, A. Klug, and R. Dominguez. 2007. Structural basis for the actin-binding function of missing-in-metastasis. *Structure*. 15:145–155.

Luo, L. 2000. Rho GTPases in neuronal morphogenesis. *Nat. Rev. Neurosci.* 1:173–180.

Mattila, P.K., A. Pykäläinen, J. Saarikangas, V.O. Paavilainen, H. Vihinen, E. Jokitalo, and P. Lappalainen. 2007. Missing-in-metastasis and IRSp53 deform $PI(4,5)P_2$-rich membranes by an inverse BAR domain–like mechanism. *J. Cell Biol.* 176:953–964.

Miki, H., and T. Takenawa. 2002. WAVE2 serves a functional partner of IRSp53 by regulating its interaction with Rac. *Biochem. Biophys. Res. Commun.* 293:93–99.

Miki, H., H. Yamaguchi, S. Suetsugu, and T. Takenawa. 2000. IRSp53 is an essential intermediate between Rac and WAVE in the regulation of membrane ruffling. *Nature*. 408:732–735.

Millard, T.H., G. Bompard, M.Y. Heung, T.R. Dafforn, D.J. Scott, L.M. Machesky, and K. Fütterer. 2005. Structural basis of filopodia formation induced by the IRSp53/MIM homology domain of human IRSp53. *EMBO J.* 24:240–250.

Nakagawa, H., H. Miki, M. Nozumi, T. Takenawa, S. Miyamoto, J. Wehland, and J.V. Small. 2003. IRSp53 is colocalised with WAVE2 at the tips of protruding lamellipodia and filopodia independently of Mena. *J. Cell Sci.* 116:2577–2583.

Nishiyama, T., T. Sasaki, K. Takaishi, M. Kato, H. Yaku, K. Araki, Y. Matsuura, and Y. Takai. 1994. *rac* p21 is involved in insulin-induced membrane ruffling and *rho* p21 is involved in hepatocyte growth factor- and 12-*O*-tetradecanoylphorbol-13-acetate (TPA)-induced membrane ruffling in KB cells. *Mol. Cell. Biol.* 14:2447–2456.

Okamura-Oho, Y., T. Miyashita, K. Ohmi, and M. Yamada. 1999. Dentatorubral-pallidoluysian atrophy protein interacts through a proline-rich region near polyglutamine with the SH3 domain of an insulin receptor tyrosine kinase substrate. *Hum. Mol. Genet*. 8:947–957.

Price, L.S., J. Leng, M.A. Schwartz, and G.M. Bokoch. 1998. Activation of Rac and Cdc42 by integrins mediates cell spreading. *Mol. Biol. Cell*. 9:1863–1871.

Ridley, A.J., H.F. Paterson, C.L. Johnston, D. Diekmann, and A. Hall. 1992. The small GTP-binding protein rac regulates growth factor-induced membrane ruffling. *Cell*. 70:401–410.

Ridley, A.J., M.A. Schwartz, K. Burridge, R.A. Firtel, M.H. Ginsberg, G. Borisy, J.T. Parsons, and A.R. Horwitz. 2003. Cell migration: integrating signals from front to back. *Science*. 302:1704–1709.

Rodley, P., N. Hatano, N.S. Nishikawa, B.C. Roy, S. Sarkar, and R. Kiyama. 2003. A differential genomic cloning for cancer study: an outline and applications. *Recent Research Developments in Molecular Biology*. 1:13–27.

Roy, B.C., T. Aoyagi, S. Sarkar, K. Nomura, H. Kanda, K. Iwaya, M. Tachibana, and R. Kiyama. 2005. Pathological characterization of Kank in renal cell carcinoma. *Exp. Mol. Pathol.* 78:41–48.

Sarkar, S., B.C. Roy, N. Hatano, T. Aoyagi, K. Gohji, and R. Kiyama. 2002. A novel ankyrin repeat-containing gene (Kank) located at 9p24 is a growth suppressor of renal cell carcinoma. *J. Biol. Chem.* 277:36585–36591.

Scita, G., J. Nordstrom, R. Carbone, P. Tenca, G. Giardina, S. Gutkind, M. Bjarnegård, C. Betsholtz, and P.P. Di Fiore. 1999. EPS8 and E3B1 transduce signals from Ras to Rac. *Nature*. 401:290–293.

Scita, G., P. Tenca, L.B. Areces, A. Tocchetti, E. Frittoli, G. Giardina, I. Ponzanelli, P. Sini, M. Innocenti, and P.P. Di Fiore. 2001. An effector region in Eps8 is responsible for the activation of the Rac-specific GEF activity of Sos-1 and for the proper localization of the Rac-based actin-polymerizing machine. *J. Cell Biol.* 154:1031–1044.

Sedgwick, S.G., and S.J. Smerdon. 1999. The ankyrin repeat: a diversity of interactions on a common structural framework. *Trends Biochem. Sci.* 24:311–316.

Soltau, M., D. Richter, and H.J. Kreienkamp. 2002. The insulin receptor substrate IRSp53 links postsynaptic shank1 to the small G-protein cdc42. *Mol. Cell. Neurosci.* 21:575–583.

Soltau, M., K. Berhörster, S. Kindler, F. Buck, D. Richter, and H.J. Kreienkamp. 2004. Insulin receptor substrate of 53 kDa links postsynaptic shank to PSD-95. *J. Neurochem.* 90:659–665.

Steffen, A., K. Rottner, J. Ehinger, M. Innocenti, G. Scita, J. Wehland, and T.E. Stradal. 2004. Sra-1 and Nap1 link Rac to actin assembly driving lamellipodia formation. *EMBO J.* 23:749–759.

Suetsugu, S., S. Kurisu, T. Oikawa, D. Yamazaki, A. Oda, and T. Takenawa. 2006a. Optimization of WAVE2 complex–induced actin polymerization by membrane-bound IRSp53, PIP_3, and Rac. *J. Cell Biol.* 173:571–585.

Suetsugu, S., K. Murayama, A. Sakamoto, K. Hanawa-Suetsugu, A. Seto, T. Oikawa, C. Mishima, M. Shirouzu, T. Takenawa, and S. Yokoyama. 2006b. The RAC binding domain/IRSp53-MIM homology domain of IRSp53 induces RAC-dependent membrane deformation. *J. Biol. Chem.* 281:35347–35358.

Takenawa, T., and H. Miki. 2001. WASP and WAVE family proteins: key molecules for rapid rearrangement of cortical actin filaments and cell movement. *J. Cell Sci.* 114:1801–1809.

Van Aelst, L., and C. D'Souza-Schorey. 1997. Rho GTPases and signaling networks. *Genes Dev.* 11:2295–2322.

Vignal, E., A. Blangy, M. Martin, C. Gauthier-Rouvière, and P. Fort. 2001. Kinectin is a key effector of RhoG microtubule-dependent cellular activity. *Mol. Cell. Biol.* 21:8022–8034.

Yamagishi, A., M. Masuda, T. Ohki, H. Onishi, and N. Mochizuki. 2004. A novel actin bundling/filopodium-forming domain conserved in insulin receptor tyrosine kinase substrate p53 and missing in metastasis protein. *J. Biol. Chem.* 279:14929–14936.

Yamazaki, M., H. Miyazaki, H. Watanabe, T. Sasaki, T. Maehama, M.A. Frohman, and Y. Kanaho. 2002. Phosphatidylinositol 4-phosphate 5-kinase is essential for ROCK-mediated neurite remodeling. *J. Biol. Chem.* 277:17226–17230.

Yang, D., F. Buchholz, Z. Huang, A. Goga, C.Y. Chen, F.M. Brodsky, and J.M. Bishop. 2002. Short RNA duplexes produced by hydrolysis with *Escherichia coli* RNase III mediate effective RNA interference in mammalian cells. *Proc. Natl. Acad. Sci. USA*. 99:9942–9947.